ELSEVIER

Comput. Methods Appl. Mech. Engrg. 169 (1999) 1–18

Computer methods in applied mechanics and engineering

A consistent co-rotational finite element formulation for geometrically nonlinear dynamic analysis of 3-D beams

Kuo Mo Hsiao*, Jer Yan Lin, Wen Yi Lin

Department of Mechanical Engineering, National Chiao Tung University, Hsinchu, Taiwan, ROC

Received 6 March 1998; revised 24 April 1998

Abstract

A co-rotational total Lagrangian finite element formulation for the geometrically nonlinear dynamic analysis of spatial Euler beam with large rotations but small strain, is presented.

The nodal coordinates, displacements, rotations, velocities, accelerations, and the equations of motion of the structure are defined in a fixed global set of coordinates. The beam element has two nodes with six degrees of freedom per node. The element nodal forces are conventional forces and moments. The kinematics of beam element are defined in terms of element coordinates, which are constructed at the current configuration of the beam element. Both the element deformation nodal forces and inertia nodal forces are systematically derived by consistent linearization of the fully geometrically nonlinear beam theory using the d'Alembert principle and the virtual work principle in the current element coordinates.

An incremental-iterative method based on the Newmark direct integration method and the Newton–Raphson method is employed here for the solution of the nonlinear equations of motion. Numerical examples are presented to demonstrate the accuracy and efficiency of the proposed method.

1. Introduction

The nonlinear dynamic behavior of beam structures, e.g. framed structures, flexible mechanisms and robot arms, has been the subject of considerable research [1–13]. Currently, the most popular approach for this analysis is to develop finite element models. The formulations, which have been used in the literature, might be divided into three categories: total Lagrangian (TL) formulation [3–10], updated Lagrangian (UL) formulation [3,9] and co-rotational (CR) formulation [1,2,11–13]. It is well known that within the co-rotating system either a TL or a UL formulation may be employed [14,15]. These formulations are consequently termed CR–TL and CR–UL formulations. The reference configuration used in a CR–TL formulation differ from the one used in a conventional TL formulation by the motion performed by the co-rotating coordinate system from the initial to the current (or neighboring) configuration. In order to capture correctly all inertia effects and coupling among bending, twisting, and stretching deformations of the beam elements, the formulation of beam elements might be derived by the fully geometrically nonlinear beam theory [5]. The exact expressions for the element inertia and deformation nodal forces, which are required in a TL formulation for large displacement/small strain problems, are highly nonlinear functions of element nodal parameters. However, the dominant factors in the geometrical nonlinearities of beam structures are attributable to finite rotations, the strains remaining small. For a beam structures discretized by finite elements, this implies that the motion of the individual elements to a large extent will consist of rigid body motion. If the rigid body motion part is eliminated from the total displacements and the element size is properly chosen, the deformational part of the motion is always small relative to the local

* Corresponding author.

0045-7825/99/$ – see front matter
PII: S0045-7825(98)00152-2

element axes; thus in conjunction with the co-rotational formulation, the higher order terms of nodal parameters in the element deformation and inertia nodal forces may be neglected by consistent linearization [5,12]. The so-called 'Natural approach' by Argyris and co-workers, for instance [16–19], is also based on the idea of separating rigid body motions from local deformations. It has been used to various application, such as linear, large displacement/small strain, and large strain problems. The co-rotational formulation has been extensively applied in the nonlinear static analysis. However, the application of co-rotational formulation in the nonlinear dynamic analysis has been rather limited (e.g. [1,2,11–13]). In [1,2], a co-rotational formulation is presented for the transient analysis of space frames in large displacement, small strain problems. To the authors' knowledge, it seems that the governing equations in [1,2] are not obtained by consistent linearization of the fully geometrically non-linear beam theory. Thus, they cannot account for the complete inertia effects and deformation coupling. In [12], Hsiao et al. presented a co-rotational finite element formulation and numerical procedure for the dynamic analysis of planar beam structures. Both the element deformation and inertia forces are systematically derived by consistent linearization of the fully geometrically nonlinear beam theory using the d'Alembert principle and the virtual work principle. This formulation and numerical procedure were proven to be very effective by numerical examples studied in [12]. However, it is only limited for planar beam structures.

The objective of this study is to present a consistent co-rotational finite element formulation and numerical procedure for the nonlinear dynamic analysis of three-dimensional elastic Euler beam using consistent linearization of the fully geometrically nonlinear beam theory. A general formulation for three-dimensional beam element is not a simple extension of a two dimensional formulation, because large rotations in three dimensional analysis are not vector quantities; that is, they do not comply with the rules of vector operations [20]. In [21] a motion process of the three-dimensional beam element is proposed for the large displacement and rotation analysis of spatial frames. In [15], Hsiao presented a co-rotational total Lagrangian formulation of beam element for the static nonlinear analysis of three-dimensional beam structures with large rotations but small strains. All coupling among bending, twisting and stretching deformations for beam element is correctly considered by the fully geometrically nonlinear beam theory. Element deformations and element equations are defined in terms of element coordinates which are constructed at the current configuration of the beam element. The element deformations are determined by three rotation parameters, which are used to determine the orientation of element cross section. In conjunction with the co-rotational formulation, the higher-order terms of nodal parameters in element nodal force and stiffness matrix are consistently dropped. It seems that this element can be extended for the nonlinear dynamic analysis of the beam structures. Thus, the beam element presented in [15] is extended and employed here.

The relation between the time derivatives of the rotation parameters proposed in [15] and the angular velocity and the angular acceleration is derived here. The beam element developed here has two nodes with six degrees of freedom per node. The element nodal forces are conventional force and moment. The element deformation and inertia nodal forces are systematically derived by using the d'Alembert principle and the virtual work principle. An incremental-iterative method based on the Newmark direct integration method and the Newton–Raphson method is employed here for the solution of the nonlinear equations of motion. Numerical examples are presented and compared with the results reported in the literature to demonstrate the accuracy and efficiency of the proposed method.

2. Finite element formulation

2.1. Basic assumptions

The following assumptions are made in derivation of the beam element behavior.

(1) The beam is prismatic and slender, and the Euler-Bernoulli hypothesis is valid.
(2) The cross section of the beam is doubly symmetric.
(3) The unit extension and the twist rate of the centroid axis of the beam element are uniform.
(4) The cross section of the beam element does not deform in its own plane and strains within this cross section can be neglected.
(5) The out-of-plane warping of the cross section is the product of the twist rate of the beam element and the Saint Venant warping function for a prismatic beam of the same cross section.

(6) The deformation displacements and rotations of the beam element are small.
(7) The strains of the beam element are small.

In conjunction with the co-rotational formulation, the sixth assumption can always be satisfied if the element size is properly chosen.

2.2. Coordinate systems

In this paper, a co-rotational total Lagrangian formulation is adopted. In order to describe the system, we define three sets of right-handed rectangular Cartesian coordinate systems:

(1) A fixed global set of coordinates, X_i $(i = 1, 2, 3)$ (see Fig. 1); the nodal coordinates, displacements, rotations, velocities and accelerations, and the equations of motion of the system are defined in these coordinates.
(2) Element cross section coordinates, x_i^S $(i = 1, 2, 3)$ (see Fig. 1); a set of element cross section coordinates is associated with each cross section of the beam element. The origin of this coordinate system is rigidly tied to the centroid of the cross section. The x_1^S axes are chosen to coincide with the normal of the unwrapped cross section and the x_2^S and x_3^S axes are chosen to be the principal directions of the cross section.
(3) Element coordinates, x_i $(i = 1, 2, 3)$ (see Fig. 1); a set of element coordinates is associated with each element, which is constructed at the current configuration of the beam element. The origin of this coordinate system is located at node 1, and the x_1 axis is chosen to pass through two end nodes of the element; the x_2 and x_3 axes are determined by the method proposed in [15,21]. *Note that this coordinate system is just a local coordinate system, which is updated at each iteration, not a moving coordinate system.* The deformations, deformation nodal forces, inertia nodal forces, stiffness matrices and inertia matrices of the elements are defined in terms of these coordinates. In this paper the element deformations are determined by the rotation of element cross section coordinate systems relative to this coordinate system.

2.3. Rotation vector and rotation parameters

For convenience of the later discussion, the term 'rotation vector' is used to represent a finite rotation. Fig. 2 shows that a vector $\boldsymbol{b}$ which as a result of the application of a rotation vector $\boldsymbol{a} = \phi \boldsymbol{e}$ is transported to the new position $\boldsymbol{b}'$. The relation between $\boldsymbol{b}'$ and $\boldsymbol{b}$ may be expressed as [22,23]

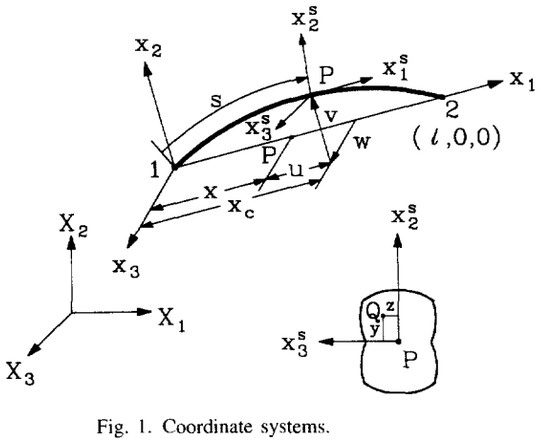

Fig. 1. Coordinate systems.

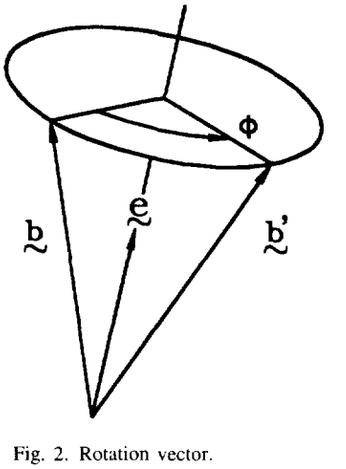

Fig. 2. Rotation vector.

$$\begin{aligned} \boldsymbol{b}' &= \boldsymbol{b}\cos\phi + (1-\cos\phi)(\boldsymbol{e}\cdot\boldsymbol{b})\boldsymbol{e} + \sin\phi(\boldsymbol{e}\times\boldsymbol{b}) \\ &= \left[\boldsymbol{I} + \frac{\sin\phi}{\phi}(\boldsymbol{a}\times\boldsymbol{I}) + \frac{1-\cos\phi}{\phi^2}\boldsymbol{a}\times(\boldsymbol{a}\times\boldsymbol{I})\right]\boldsymbol{b} \\ &= \boldsymbol{R}\boldsymbol{b} \end{aligned} \tag{1}$$

where ϕ is the angle of rotation about the axis of rotation as shown in Fig. 1, $\boldsymbol{e}$ is the unit vector along the axis of rotation, $\boldsymbol{I}$ is the identity matrix of order 3×3, and $\boldsymbol{R}$ is the so-called rotation matrix.

In this paper, the symbol $(\dot{\ })$ denotes time derivative. The time derivative of Eq. (1) may be expressed as

$$\frac{\mathrm{d}\boldsymbol{b}'}{\mathrm{d}t} = \dot{\boldsymbol{R}}\boldsymbol{b} = \dot{\boldsymbol{R}}\boldsymbol{R}^{\mathrm{t}}\boldsymbol{b}' = (\boldsymbol{\omega}\times\boldsymbol{I})\boldsymbol{b}' \tag{2}$$

where $\boldsymbol{\omega}$ is the angular velocity vector. From Eqs. (1) and (2), the relation between $\boldsymbol{\omega}$ and $\dot{\boldsymbol{a}}$, the time derivative of the rotation vector $\boldsymbol{a}$, may be expressed by [23]

$$\begin{aligned} &\boldsymbol{\omega} = \Gamma(\boldsymbol{a})\dot{\boldsymbol{a}} \\ &\Gamma(\boldsymbol{a}) = [\boldsymbol{I} + p(\boldsymbol{a}\times\boldsymbol{I}) + q\boldsymbol{a}\times(\boldsymbol{a}\times\boldsymbol{I})] \end{aligned} \tag{3}$$

where

$$p = \frac{1-\cos\phi}{\phi^2}, \quad \text{and} \quad q = \frac{1}{\phi^2}\left(1 - \frac{\sin\phi}{\phi}\right).$$

The virtual rotation $\delta\boldsymbol{\varphi}$ is related to $\delta\boldsymbol{a}$, the virtual change of the rotation vector $\boldsymbol{a}$, through the same relationship that exists between $\boldsymbol{\omega}$ and $\dot{\boldsymbol{a}}$ [23] i.e.:

$$\delta\boldsymbol{\varphi} = \Gamma(\boldsymbol{a})\,\delta\boldsymbol{a} \tag{4}$$

where $\delta\boldsymbol{\varphi} = \{\delta\varphi_1, \delta\varphi_2, \delta\varphi_3\}$, $\delta\varphi_i$ $(i = 1, 2, 3)$ are virtual rotation about x_i axes. In this paper, the symbol $\{\ \}$ denotes column matrix.

The time derivative of Eq. (3) may be expressed by

$$\begin{aligned} &\dot{\boldsymbol{\omega}} = \dot{\Gamma}(\boldsymbol{a})\dot{\boldsymbol{a}} + \Gamma(\boldsymbol{a})\ddot{\boldsymbol{a}} \\ &\dot{\Gamma}(\boldsymbol{a}) = \dot{p}(\boldsymbol{a}\times\boldsymbol{I}) + \dot{q}\boldsymbol{a}\times(\boldsymbol{a}\times\boldsymbol{I}) + p(\dot{\boldsymbol{a}}\times\boldsymbol{I}) + q\dot{\boldsymbol{a}}\times(\boldsymbol{a}\times\boldsymbol{I}) + q\boldsymbol{a}\times(\dot{\boldsymbol{a}}\times\boldsymbol{I}) \end{aligned} \tag{5}$$

where $\dot{\boldsymbol{\omega}}$ is the angular acceleration, $\ddot{\boldsymbol{a}}$ is the second time derivative of $\boldsymbol{a}$.

From Eqs. (3) and (5), it can be seen that $\Gamma(\boldsymbol{0}) = \boldsymbol{I}$ and $\dot{\Gamma}(\boldsymbol{0}) = \boldsymbol{0}$. Thus, $\boldsymbol{\omega} = \dot{\boldsymbol{a}}$, $\delta\boldsymbol{\varphi} = \delta\boldsymbol{a}$ and $\dot{\boldsymbol{\omega}} = \ddot{\boldsymbol{a}}$, when $\boldsymbol{a} = \boldsymbol{0}$.

Let $\boldsymbol{e}_i$ and $\boldsymbol{e}_i^S$ $(i = 1, 2, 3)$ denote the unit vectors associated with the x_i and x_i^S axes, respectively. Here, the traid $\boldsymbol{e}_i^S$ in the deformed state is assumed to be achieved by the successive application of the following two rotation vectors to the traid $\boldsymbol{e}_i$:

$$\boldsymbol{\theta}_n = \theta_n\boldsymbol{n} \tag{6}$$

$$\boldsymbol{\theta}_t = \theta_1\boldsymbol{t} \tag{7}$$

where

$$\begin{aligned} \boldsymbol{n} &= \{0, \theta_2/(\theta_2^2+\theta_3^2)^{1/2}, \theta_3/(\theta_2^2+\theta_3^2)^{1/2}\} \\ &= \{0, n_2, n_3\} \end{aligned} \tag{8}$$

$$\boldsymbol{t} = \{\cos\theta_n, \theta_2, \theta_3\} \tag{9}$$

$$\cos\theta_n = (1-\theta_2^2-\theta_3^2)^{1/2} \tag{10}$$

$$\theta_2 = -\frac{\mathrm{d}w(s)}{\mathrm{d}s}, \qquad \theta_3 = \frac{\mathrm{d}v(s)}{\mathrm{d}s} \tag{11}$$

in which $\boldsymbol{n}$ is the unit vector perpendicular to the vectors $\boldsymbol{e}_1$ and $\boldsymbol{e}_1^S$, and $\boldsymbol{t}$ is the tangent unit vector of the deformed centroid axis of the beam element. Note that $\boldsymbol{e}_1^S$ coincides with $\boldsymbol{t}$. θ_n is the inverse of $\cos\theta_n$. $v(s)$ and

$w(s)$ are the lateral deflections of the centroid axis of the beam element in the x_2 and x_3 directions, respectively, and s is the arc length of the deformed centroid axis.

Using Eqs. (1) and (6)–(10), the relation between the vectors $\boldsymbol{e}_i$ and $\boldsymbol{e}_i^S$ $(i = 1, 2, 3)$ in the element coordinate system may be obtained as [15]

$$\boldsymbol{e}_i^S = [\boldsymbol{t}, \boldsymbol{R}_1, \boldsymbol{R}_2]\boldsymbol{e}_i = \boldsymbol{R}_\theta \boldsymbol{e}_i \tag{12}$$

$$\boldsymbol{R}_1 = \cos\theta_1 \boldsymbol{r}_1 + \sin\theta_1 \boldsymbol{r}_2\,, \quad \boldsymbol{R}_2 = -\sin\theta_1 \boldsymbol{r}_1 + \cos\theta_1 \boldsymbol{r}_2$$

$$\boldsymbol{r}_1 = \{-\theta_3, \cos\theta_n + (1-\cos\theta_n)n_2^2, (1-\cos\theta_n)n_2 n_3\}$$

$$\boldsymbol{r}_2 = \{\theta_2, (1-\cos\theta_n)n_2 n_3, \cos\theta_n + (1-\cos\theta_n)n_3^2\} \tag{13}$$

where $\boldsymbol{R}_\theta$ is a rotation matrix. The rotation matrix is determined by θ_i $(i = 1, 2, 3)$. Thus, θ_i are called rotation parameters in this study.

Let $\boldsymbol{\theta} = \{\theta_1, \theta_2, \theta_3\}$ be the column matrix of rotation parameters, $\delta\boldsymbol{\theta}$ be the variation of $\boldsymbol{\theta}$. The traid $\boldsymbol{e}_i^S$ $(i = 1, 2, 3)$ corresponding to $\boldsymbol{\theta} + \delta\boldsymbol{\theta}$ may be achieved by the application of $\delta\varphi_i$ $(i = 1, 2, 3)$, the virtual rotation about x_i axes, to the traid $\boldsymbol{e}_i^S$ $(i = 1, 2, 3)$ corresponding to $\boldsymbol{\theta}$ [15]. When θ_2 and θ_3 are much smaller than unity, the relationship between $\delta\boldsymbol{\theta}$ and $\delta\boldsymbol{\varphi} = \{\delta\varphi_1, \delta\varphi_2, \delta\varphi_3\}$ may be approximated by [15]

$$\delta\boldsymbol{\theta} = \begin{bmatrix} 1 & \theta_3/2 & -\theta_2/2 \\ -\theta_3 & 1 & 0 \\ \theta_2 & 0 & 1 \end{bmatrix} \delta\boldsymbol{\varphi} = \boldsymbol{T}^{-1}\,\delta\boldsymbol{\varphi}\,. \tag{14}$$

The time derivative of $\boldsymbol{\theta}$ is related to angular velocity $\boldsymbol{\omega}$ through the same relationship that exists between $\delta\boldsymbol{\theta}$ and $\delta\boldsymbol{\varphi}$ i.e.:

$$\dot{\boldsymbol{\theta}} = \boldsymbol{T}^{-1}\boldsymbol{\omega} \tag{15}$$

The time derivative of Eq. (15) may be expressed by

$$\ddot{\boldsymbol{\theta}} = \boldsymbol{T}^{-1}\dot{\boldsymbol{\omega}} + \dot{\boldsymbol{T}}^{-1}\boldsymbol{\omega} \tag{16}$$

2.4. Nodal parameters and forces

The global nodal parameters for the system of equations corresponding to the element local nodes j $(j = 1, 2)$ are U_{ij}, the X_i $(i = 1, 2, 3)$ components of the translation vectors $\boldsymbol{U}_j$ at nodes j, and Φ_{ij}, the X_i $(i = 1, 2, 3)$ components of the rotation vectors $\boldsymbol{\Phi}_j$ at nodes j. *Note that here, the values of $\boldsymbol{\Phi}_j$ are reset to zero at current configuration. Thus, $\delta\Phi_{ij}$, the variation of Φ_{ij}, represents infinitesimal rotations about the X_i axes (see Eq. (4)), and the values of $\dot{\boldsymbol{\Phi}}_j$ and $\ddot{\boldsymbol{\Phi}}_j$ are equal to the values of the angular velocity vectors and angular acceleration vectors at nodes j (see Eqs. (3) and (5)), respectively.* The generalized nodal forces corresponding to $\delta\Phi_{ij}$ are the conventional moments about the X_i axes. The generalized nodal forces corresponding to δU_{ij}, the variation of U_{ij}, are the forces in the X_i directions.

The element proposed in [15] is employed and extended here. The element has two nodes with six degrees of freedom per node. Two sets of element nodal parameters termed 'explicit nodal parameters' and 'implicit nodal parameters' are employed. The explicit nodal parameters of the element are used for the assembly of the system equations from the element equations. Thus, they should be consistent with the global nodal parameters, and are chosen to be u_{ij}, the x_i $(i = 1, 2, 3)$ components of the translation vectors $\boldsymbol{u}_j$ at node j $(j = 1, 2)$ and ϕ_{ij}, the x_i $(i = 1, 2, 3)$ components of the rotation vectors $\boldsymbol{\phi}_j$ at node j $(j = 1, 2)$. *Note that here, the values of $\boldsymbol{\phi}_j$ are reset to zero at current configuration. Thus, $\delta\phi_{ij}$, the variation of ϕ_{ij}, represents infinitesimal rotations about the x_i axes (see Eq. (4)), and the values of $\dot{\boldsymbol{\phi}}_j$ and $\ddot{\boldsymbol{\phi}}_j$ are equal to the values of the angular velocity vectors and angular acceleration vectors at nodes j (see Eqs. (3) and (5)), respectively.* The generalized nodal forces corresponding to $\delta\phi_{ij}$ are m_{ij}, the conventional moments about the x_i axes. The generalized nodal forces corresponding to δu_{ij}, the variation of u_{ij}, are f_{ij}, the forces in the x_j directions.

The implicit nodal parameters of the element are used to determine the deformation of the beam element. They are chosen to be u_{ij}, the x_i $(i = 1, 2, 3)$ components of the translation vectors $\boldsymbol{u}_j$ at node j $(j = 1, 2)$ and θ_{ij}, the nodal values of the rotation parameters θ_i $(i = 1, 2, 3)$ at node j $(j = 1, 2)$. The generalized nodal forces

corresponding to δu_{ij} and $\delta\theta_{ij}$ are f_{ij} and m_{ij}^{θ}, the forces in the x_i directions and the generalized moments, respectively. *Note that m_{ij}^{θ} are not conventional moments, because $\delta\theta_{ij}$ are not infinitesimal rotations about the x_i axes at deformed state.*

In view of Eq. (14), the relations between the variation of the implicit and explicit nodal parameters may be expressed as

$$\delta \boldsymbol{q}_{\theta} = \begin{Bmatrix} \delta \boldsymbol{u}_1 \\ \delta \boldsymbol{\theta}_1 \\ \delta \boldsymbol{u}_2 \\ \delta \boldsymbol{\theta}_2 \end{Bmatrix} = \begin{bmatrix} \boldsymbol{I} & \boldsymbol{0} & \boldsymbol{0} & \boldsymbol{0} \\ \boldsymbol{0} & \boldsymbol{T}_1^{-1} & \boldsymbol{0} & \boldsymbol{0} \\ \boldsymbol{0} & \boldsymbol{0} & \boldsymbol{I} & \boldsymbol{0} \\ \boldsymbol{0} & \boldsymbol{0} & \boldsymbol{0} & \boldsymbol{T}_2^{-1} \end{bmatrix} \begin{Bmatrix} \delta \boldsymbol{u}_1 \\ \delta \boldsymbol{\phi}_1 \\ \delta \boldsymbol{u}_2 \\ \delta \boldsymbol{\phi}_2 \end{Bmatrix} = \boldsymbol{T}_{\theta\phi}\, \delta \boldsymbol{q} \tag{17}$$

where $\delta \boldsymbol{u}_j = \{\delta u_{1j}, \delta u_{2j}, \delta u_{3j}\}$, $\delta \boldsymbol{\theta}_j = \{\delta\theta_{1j}, \delta\theta_{2j}, \delta\theta_{3j}\}$ and $\delta \boldsymbol{\phi}_j = \{\delta\phi_{1j}, \delta\phi_{2j}, \delta\phi_{3j}\}$, $(j = 1, 2)$; $\boldsymbol{I}$ and $\boldsymbol{0}$ are the identity and zero matrices of order 3×3, respectively; $\boldsymbol{T}_j^{-1}$ $(j = 1, 2)$ are nodal values of $\boldsymbol{T}^{-1}$ given in Eq. (14).

Let $\boldsymbol{f} = \{\boldsymbol{f}_1, \boldsymbol{m}_1, \boldsymbol{f}_2, \boldsymbol{m}_2\}$, $\boldsymbol{f}_{\theta} = \{\boldsymbol{f}_1, \boldsymbol{m}_1^{\theta}, \boldsymbol{f}_2, \boldsymbol{m}_2^{\theta}\}$, where $\boldsymbol{f}_j = \{f_{1j}, f_{2j}, f_{3j}\}$, $\boldsymbol{m}_j = \{m_{1j}, m_{2j}, m_{3j}\}$, and $\boldsymbol{m}_j^{\theta} = \{m_{1j}^{\theta}, m_{2j}^{\theta}, m_{3j}^{\theta}\}$ $(j = 1, 2)$, denote the internal nodal force vectors corresponding to the variation of the explicit and implicit nodal parameters, $\delta \boldsymbol{q}$ and $\delta \boldsymbol{q}_{\theta}$, respectively. Using the contragradient law [24] and Eq. (17), the relation between $\boldsymbol{f}$ and $\boldsymbol{f}_{\theta}$, may be given by

$$\boldsymbol{f} = \boldsymbol{T}_{\theta\phi}^{\mathrm{t}} \boldsymbol{f}_{\theta}\,. \tag{18}$$

2.5. Kinematics of beam element

The deformations of the beam element are described in the current element coordinate system. From the kinematic assumptions made in this paper, the deformations of the beam element may be determined by the displacements of the centroid axis of the beam element, orientation of the cross section (element cross section coordinates), and the out-of-plane warping of the cross section. Let Q (Fig. 1) be an arbitrary point in the beam element, and P be the point corresponding to Q on the centroid axis. The position vector of point Q in the undeformed and deformed configurations may be expressed as

$$\boldsymbol{r}_0 = x\boldsymbol{e}_1 + y\boldsymbol{e}_2 + z\boldsymbol{e}_3 \tag{19}$$

$$\boldsymbol{r} = x_c(s)\boldsymbol{e}_1 + v(s)\boldsymbol{e}_2 + w(s)\boldsymbol{e}_3 + \theta_{1,s}\boldsymbol{e}_1^s + y\boldsymbol{e}_2^s + z\boldsymbol{e}_3^s \tag{20}$$

where $x_c(s)$, $v(s)$ and $w(s)$ are the x_1, x_2 and x_3 coordinates of point P, respectively, s is the arc length of the deformed centroid axis measured from node 1 to point P. The relationship among $x_c(s)$, $v(s)$, $w(s)$ and s may be given as

$$x_c(s) = u_{11} + \int_0^s \cos\theta_n \, \mathrm{d}s \tag{21}$$

where u_{11} is the displacement of node 1 in the x_1 direction, and $\cos\theta_n$ is defined in Eq. (10). Note that due to the definition of the element coordinate system, the value of u_{11} is equal to zero. However, the variation and time derivatives of u_{11} are not zero. Making use of Eq. (21), one obtains

$$S = \frac{2\ell}{\displaystyle\int_{-1}^{1} \cos\theta_n \, \mathrm{d}\xi} \tag{22}$$

$$\ell = x_c(S) - x_c(0) = L - u_{11} + u_{12} \tag{23}$$

$$\xi = -1 + \frac{2s}{S} \tag{24}$$

in which S and ℓ are the current arc length and chord length of the centroid axis of the beam element, respectively, L is the length of the undeformed beam axis, and u_{12} is the displacement of node 2 in the x_1 direction.

Here, the lateral deflections of the centroid axis $v(s)$ and $w(s)$ are assumed to be the Hermitian polynomials of

s, and the rotation about the centroid axis $\theta_1(s)$ (Eq. (7)) is assumed to be linear polynomials of s. $v(s)$, $w(s)$ and $\theta_1(s)$ may be expressed by

$$\begin{aligned} v(s) &= \{N_1, N_2, N_3, N_4\}^{\mathrm{t}}\{u_{21}, \theta_{31}, u_{22}, \theta_{32}\} = \boldsymbol{N}_b^{\mathrm{t}}\boldsymbol{u}_b \\ w(s) &= \{N_1, -N_2, N_3, -N_4\}^{\mathrm{t}}\{u_{31}, \theta_{21}, u_{32}, \theta_{22}\} = \boldsymbol{N}_c^{\mathrm{t}}\boldsymbol{u}_c \\ \theta_1(s) &= \{N_5, N_6\}^{\mathrm{t}}\{\theta_{11}, \theta_{12}\} = \boldsymbol{N}_d^{\mathrm{t}}\boldsymbol{u}_d \end{aligned} \tag{25}$$

where u_{2j} and u_{3j} ($j = 1, 2$) are nodal values of v and w at nodes j, respectively, and θ_{ij} ($i = 1, 2, 3$, $j = 1, 2$) are nodal values of θ_i at nodes j. Note that, due to the definition of the element coordinates, the values of u_{2j} and u_{3j} ($j = 1, 2$) are zero. However, their variations and time derivatives are not zero. N_i ($i = 1$–6) are shape functions and are given by

$$\begin{aligned} N_1 &= \frac{1}{4}(1-\xi)^2(2+\xi), \qquad N_2 = \frac{S}{8}(1-\xi^2)(1-\xi), \\ N_3 &= \frac{1}{4}(1+\xi)^2(2-\xi), \qquad N_4 = \frac{S}{8}(-1+\xi^2)(1+\xi), \\ N_5 &= \frac{1}{2}(1-\xi), \qquad N_6 = \frac{1}{2}(1+\xi). \end{aligned} \tag{26}$$

The axial displacements of the centroid axis may be determined from the lateral deflections of the centroid axis and Eqs. (21)–(24).

If x, y and z in Eq. (19) are regarded as the lagrangian coordinates, the Green strains ε_{11} ε_{12} and ε_{13} are given by [25]

$$\begin{aligned} \varepsilon_{11} &= \frac{1}{2}(\boldsymbol{r}_{,x}^{\mathrm{t}}\boldsymbol{r}_{,x} - 1) \\ \varepsilon_{12} &= \frac{1}{2}\boldsymbol{r}_{,x}^{\mathrm{t}}\boldsymbol{r}_{,y} \\ \varepsilon_{13} &= \frac{1}{2}\boldsymbol{r}_{,x}^{\mathrm{t}}\boldsymbol{r}_{,z}. \end{aligned} \tag{27}$$

Using the chain rule for differentiation, $\boldsymbol{r}_{,x}$ in Eq. (27) may be expressed as

$$\boldsymbol{r}_{,x} = \boldsymbol{r}_{,s}(1+\varepsilon_0) \tag{28}$$

$$\varepsilon_0 = \frac{\partial s}{\partial x} - 1 \tag{29}$$

where ε_0 is the unit extension of the centroid axis. Making use of the assumption of uniform unit extension, one may rewrite Eq. (29) as

$$\varepsilon_0 = \frac{S}{L} - 1. \tag{30}$$

Substituting Eqs. (9)–(13), (20), and (28) into Eq. (27), ε_{11}, ε_{12} and ε_{13} can be calculated. ε_{11}, ε_{12} and ε_{13} are given in [15] and are not repeated here.

2.6. Element nodal force vector

The element nodal force vector $\boldsymbol{f}_\theta$ (Eq. (18)) corresponding to the implicit nodal parameters are obtained from the d'Alembert principle and the virtual work principle in the current element coordinates. For convenience, the implicit nodal parameters are divided into four generalized nodal displacement vectors $\boldsymbol{u}_i$ ($i = a, b, c, d$), where

$$\boldsymbol{u}_a = \{u_{11}, u_{12}\} \tag{31}$$

and $\boldsymbol{u}_b$, $\boldsymbol{u}_c$ and $\boldsymbol{u}_d$ are defined in Eq. (25).

The generalized force vectors corresponding to $\delta\boldsymbol{u}_i$, the variation of $\boldsymbol{u}_i$ ($i = a, b, c, d$) are

$$\begin{aligned} \boldsymbol{f}_a &= \boldsymbol{f}_a^d + \boldsymbol{f}_a^i = \{f_{11}, f_{12}\} \\ \boldsymbol{f}_b &= \boldsymbol{f}_b^d + \boldsymbol{f}_b^i = \{f_{21}, m_{31}^\theta, f_{22}, m_{32}^\theta\} \\ \boldsymbol{f}_c &= \boldsymbol{f}_c^d + \boldsymbol{f}_c^i = \{f_{31}, m_{21}^\theta, f_{32}, m_{22}^\theta\} \\ \boldsymbol{f}_d &= \boldsymbol{f}_d^d + \boldsymbol{f}_d^i = \{m_{11}^\theta, m_{12}^\theta\} \end{aligned} \tag{32}$$

where $\boldsymbol{f}_j^d$ and $\boldsymbol{f}_j^i$ $(j = a, b, c, d)$ are the deformation nodal force vectors and the inertia nodal force vectors, respectively.

The virtual work principle requires that

$$\delta\boldsymbol{u}_a^{\mathrm{t}}\boldsymbol{f}_a + \delta\boldsymbol{u}_b^{\mathrm{t}}\boldsymbol{f}_b + \delta\boldsymbol{u}_c^{\mathrm{t}}\boldsymbol{f}_c + \delta\boldsymbol{u}_d^{\mathrm{t}}\boldsymbol{f}_d = \int_V (\sigma_{11}\,\delta\varepsilon_{11} + 2\sigma_{12}\,\delta\varepsilon_{12} + 2\sigma_{13}\,\delta\varepsilon_{13} + \rho\,\delta\boldsymbol{r}^{\mathrm{t}}\ddot{\boldsymbol{r}})\,\mathrm{d}V \tag{33}$$

where V is the volume of the undeformed beam, $\delta\varepsilon_{1j}$ $(j = 1, 2, 3)$ are the variation of ε_{1j} in Eq. (27), respectively, with respect to the implicit nodal parameters. σ_{1j} $(j = 1, 2, 3)$ are the second Piola–Kirchhoff stress. For linear elastic material, the following constitutive equations are used:

$$\sigma_{11} = E\varepsilon_{11}, \qquad \sigma_{12} = 2G\varepsilon_{12} \quad \text{and} \quad \sigma_{13} = 2G\varepsilon_{13} \tag{34}$$

where E is the Young's modulus and G is shear modulus. ρ is the density, $\delta\boldsymbol{r}$ and $\ddot{\boldsymbol{r}}$ are the variation and the second-time derivative of $\boldsymbol{r}$ in Eq. (20), respectively.

It should be mentioned again that *the element coordinate system is a local coordinate system, which is updated at each iteration, not a moving coordinate system. Thus, $\ddot{\boldsymbol{r}}$ is the absolute acceleration and $\int_V \rho\,\delta\boldsymbol{r}^{\mathrm{t}}\ddot{\boldsymbol{r}}\,\mathrm{d}V$ comprises all the virtual inertia forces.*

If the element size is chosen small enough, the values of the nodal parameters (displacements and rotation parameters) of the element defined in the current element coordinate system may always be much smaller than unity. Thus, the higher-order terms of nodal parameters in the element internal nodal forces may be neglected by consistent linearization [5,12]. However, in order to include the nonlinear coupling among the bending, twisting and stretching deformations, the terms up to the second order of nodal parameters are retained in element deformation nodal forces $\boldsymbol{f}_j^d$ $(j = a, b, c, d)$. Because the values of the nodal parameters of the element may always be much smaller than unity, it is reasonable to assume that the coupling between the nodal parameters and their time derivatives are negligible. Thus, only zeroth order terms of nodal parameters are retained in element inertia nodal forces $\boldsymbol{f}_j^i$ $(j = a, b, c, d)$. Note that because the shape functions given in Eq. (26) are functions of S, the current arc length of the beam element, the variations and time derivatives of the shape functions are considered here.

Substituting Eqs. (23)–(30), and (34) into Eq. (33), and using consistent linearization, $\boldsymbol{f}_j^d$ and $\boldsymbol{f}_j^i$ $(j = a, b, c, d)$, the element deformation nodal force vectors and the element inertia nodal force vectors, respectively, may be given by

$$\begin{aligned} \boldsymbol{f}_a^d = \boldsymbol{G}_a\Big[& AE(\varepsilon_0 + \frac{3}{2}\varepsilon_0^2) + EI_z \int \Big(\frac{5}{2}\theta_{3,s}^2 - \theta_{3,s}\theta_{3,s}^*\Big)\,\mathrm{d}s \\ & + EI_y \int \Big(\frac{5}{2}\theta_{2,s}^2 - \theta_{2,s}\theta_{2,s}^*\Big)\,\mathrm{d}s + \frac{1}{2}EI_p \int \theta_{1,s}^2\,\mathrm{d}s\Big] \end{aligned} \tag{35}$$

$$\begin{aligned} \boldsymbol{f}_b^d = {} & f_{12}^d(1 + \varepsilon_0)\boldsymbol{G}_b + EI_z(1 + 4\varepsilon_0)\int \boldsymbol{N}_b''\theta_{3,s}\,\mathrm{d}s - E(I_z - I_y)\int \boldsymbol{N}_b''\theta_1\theta_{2,s}\,\mathrm{d}s \\ & - \frac{GJ}{2}\int \boldsymbol{N}_b''\theta_{1,s}\theta_2\,\mathrm{d}s + \frac{GJ}{2}\int \boldsymbol{N}_b'\theta_{1,s}\theta_{2,s}\,\mathrm{d}s \end{aligned} \tag{36}$$

$$\begin{aligned} \boldsymbol{f}_c^d = {} & f_{12}^d(1 + \varepsilon_0)\boldsymbol{G}_c + EI_y(1 + 4\varepsilon_0)\int \boldsymbol{N}_c''\theta_{2,s}\,\mathrm{d}s - E(I_z - I_y)\int \boldsymbol{N}_c''\theta_1\theta_{3,s}\,\mathrm{d}s \\ & - \frac{GJ}{2}\int \boldsymbol{N}_c''\theta_{1,s}\theta_3\,\mathrm{d}s + \frac{GJ}{2}\int \boldsymbol{N}_c'\theta_{1,s}\theta_{3,s}\,\mathrm{d}s \end{aligned} \tag{37}$$

$$f_d^i = GJ(1+\varepsilon_0)\int N'_d\theta_{1,s}\,\mathrm{d}s - \frac{GJ}{2}\int N'_d(\theta_2\theta_{3,s}-\theta_3\theta_{2,s})\,\mathrm{d}s$$
$$- E(I_z-I_y)\int N'_d\theta_{2,s}\theta_{3,s}\,\mathrm{d}s + EI_p\varepsilon_0\int N'_d\theta_{1,s}\,\mathrm{d}s \tag{38}$$

$$f_a^i = \frac{\rho AL}{2}\int_{-1}^{1} N_aN_a^{\mathrm{t}}\,\mathrm{d}\xi\,\ddot{\boldsymbol{u}}_a + \frac{\rho AL}{2}\int_{-1}^{1} N_a\left[\frac{L(1+\xi)}{4}\int_{-1}^{1}(N'_b\dot{\boldsymbol{u}}_b)^2+(N'^{\mathrm{t}}_c\dot{\boldsymbol{u}}_c)^2\,\mathrm{d}\xi\right.$$
$$\left.-\frac{L}{2}\int_{-1}^{\xi}(N'^{\mathrm{t}}_b\dot{\boldsymbol{u}}_b)^2+(N'^{\mathrm{t}}_c\dot{\boldsymbol{u}}_c)^2\,\mathrm{d}\xi\right]\mathrm{d}\xi \tag{39}$$

$$f_b^i = \frac{\rho AL}{2}\int_{-1}^{1} N_bN_b^{\mathrm{t}}\,\mathrm{d}\xi\,\ddot{\boldsymbol{u}}_b + \frac{\rho I_zL}{2}\int_{-1}^{1} N'_bN'^{\mathrm{t}}_b\,\mathrm{d}\xi\,\ddot{\boldsymbol{u}}_b + \rho AG_a^{\mathrm{t}}\dot{\boldsymbol{u}}_a\int_{-1}^{1} N_bN_c^{\mathrm{t}}\,\mathrm{d}\xi\,\dot{\boldsymbol{u}}_b$$
$$-\rho I_zG_a^{\mathrm{t}}\dot{\boldsymbol{u}}_a\int_{-1}^{1} N'_bN_f^{\mathrm{t}}\,\mathrm{d}\xi\,\dot{\boldsymbol{u}}_b + \rho I_zL\int_{-1}^{1} N'_b(N_d^{\mathrm{t}}\dot{\boldsymbol{u}}_d)(N'^{\mathrm{t}}_c\dot{\boldsymbol{u}}_c)\,\mathrm{d}\xi \tag{40}$$

$$f_c^i = \frac{\rho AL}{2}\int_{-1}^{1} N_cN_c^{\mathrm{t}}\,\mathrm{d}\xi\,\ddot{\boldsymbol{u}}_c + \frac{\rho I_yL}{2}\int_{-1}^{1} N'_cN'^{\mathrm{t}}_c\,\mathrm{d}\xi\,\ddot{\boldsymbol{u}}_c - \rho AG_a^{\mathrm{t}}\dot{\boldsymbol{u}}_a\int_{-1}^{1} N_cN_e^{\mathrm{t}}\,\mathrm{d}\xi\,\dot{\boldsymbol{u}}_c$$
$$-\rho I_yG_a^{\mathrm{t}}\dot{\boldsymbol{u}}_a\int_{-1}^{1} N'_cN_f^{\mathrm{t}}\,\mathrm{d}\xi\,\dot{\boldsymbol{u}}_c - \rho I_yL\int_{-1}^{1} N'_c(N_d^{\mathrm{t}}\dot{\boldsymbol{u}}_d)(N'^{\mathrm{t}}_b\dot{\boldsymbol{u}}_b)\,\mathrm{d}\xi \tag{41}$$

$$f_d^i = \frac{\rho I_pL}{2}\int_{-1}^{1} N_dN_d^{\mathrm{t}}\,\mathrm{d}\xi\,\ddot{\boldsymbol{u}}_d - \frac{\rho L(I_z-I_y)}{2}\int_{-1}^{1} N_d(N'^{\mathrm{t}}_b\dot{\boldsymbol{u}}_b)(N'^{\mathrm{t}}_c\dot{\boldsymbol{u}}_c)\,\mathrm{d}\xi$$
$$+\underline{\frac{\rho LJ_\omega}{S^2}G_d(G_d^{\mathrm{t}}\ddot{\boldsymbol{u}}_d) - \frac{2\rho J_\omega}{S^2}G_d(G_a^{\mathrm{t}}\dot{\boldsymbol{u}}_a)(G_d^{\mathrm{t}}\dot{\boldsymbol{u}}_d)} \tag{42}$$

where the range of integration for the integral $\int(\,)\,\mathrm{d}s$ in Eqs. (35)–(38) is from 0 to S, A is the cross-section area, N_j $(j=b,c,d)$ are given in Eq. (26), $(\,)' = \mathrm{d}(\,)/\mathrm{d}s$, $G_a = G_d = \{-1, 1\}$,

$$G_b = \frac{L}{2}\int_{-1}^{1} N'_b\theta_3\,\mathrm{d}\xi\,, \qquad G_c = \frac{-L}{2}\int_{-1}^{1} N'_c\theta_2\,\mathrm{d}\xi\,, \qquad \theta^*_{3,s} = \{2N''_1, N''_2, 2N''_3, N''_4\}^{\mathrm{t}}\boldsymbol{u}_b\,,$$
$$\theta^*_{2,s} = -\{2N''_1, -N''_2, 2N''_3, -N''_4\}^{\mathrm{t}}\boldsymbol{u}_c\,, \qquad N_a = N_d\,, \qquad N_e = \{0, N_2, 0, N_4\}\,, \qquad N_f = \{N'_1, 0, N'_3, 0\}\,,$$
$$I_y = \int z^2\,\mathrm{d}A\,, \qquad I_z = \int y^2\,\mathrm{d}A\,, \qquad I_p = I_y + I_z\,, \qquad J = \int[(-z+\omega_{,y})^2 + (y+\omega_{,z})^2]\,\mathrm{d}A\,,$$
$$J_\omega = \int \omega^2\,\mathrm{d}A\,.$$

Note that in order to compare numerical results of the present study with those given in the literature, the underlined terms in Eq. (42) are not considered in numerical studies here.

The element nodal force vector $\boldsymbol{f}$ (Eq. (18)) corresponding to the explicit nodal parameters may be obtained from Eqs. (18) and (35)–(42).

2.7. Element stiffness matrices and inertia matrices

The element stiffness matrix and inertia matrix corresponding to the explicit nodal parameters may be obtained by differentiating the element nodal force vector $\boldsymbol{f}$ in Eq. (18) with respect to explicit nodal parameters and their time derivatives. However, element matrices are used only to obtain predictors and correctors for incremental solutions of nonlinear equations of motion in this study. Thus, approximate element matrices can meet these requirements. The element stiffness matrices and consistent mass matrices of the conventional beam and bar elements [24,26] are used here and may be given by

Stiffness matrices:

$$\boldsymbol{K}_{\alpha\alpha} = \frac{AE}{L}\boldsymbol{G}_a\boldsymbol{G}_a^{\mathrm{t}} \tag{43}$$

$$\boldsymbol{K}_{bb} = \frac{EI_zL}{2}\int_{-1}^{1}\boldsymbol{N}_b''\boldsymbol{N}_b''^{\mathrm{t}}\,\mathrm{d}\xi + \frac{f_{12}^dL}{2}\int_{-1}^{1}\boldsymbol{N}_b'\boldsymbol{N}_b'^{\mathrm{t}}\,\mathrm{d}\xi \tag{44}$$

$$\boldsymbol{K}_{cc} = \frac{EI_yL}{2}\int_{-1}^{1}\boldsymbol{N}_c''\boldsymbol{N}_c''^{\mathrm{t}}\,\mathrm{d}\xi + \frac{f_{12}^dL}{2}\int_{-1}^{1}\boldsymbol{N}_c'\boldsymbol{N}_c'^{\mathrm{t}}\,\mathrm{d}\xi \tag{45}$$

$$\boldsymbol{K}_{dd} = \frac{GJ}{L}\boldsymbol{G}_d\boldsymbol{G}_d^{\mathrm{t}} \tag{46}$$

Mass matrices:

$$\boldsymbol{M}_{aa} = \rho A\int_{-1}^{1}\boldsymbol{N}_a\boldsymbol{N}_a^{\mathrm{t}}\,\mathrm{d}\xi \tag{47}$$

$$\boldsymbol{M}_{bb} = \rho A\int_{-1}^{1}\boldsymbol{N}_b\boldsymbol{N}_b^{\mathrm{t}}\,\mathrm{d}\xi + \rho I_z\int_{-1}^{1}\boldsymbol{N}_b'\boldsymbol{N}_b'^{\mathrm{t}}\,\mathrm{d}\xi \tag{48}$$

$$\boldsymbol{M}_{cc} = \rho A\int_{-1}^{1}\boldsymbol{N}_c\boldsymbol{N}_c^{\mathrm{t}}\,\mathrm{d}\xi + \rho I_y\int_{-1}^{1}\boldsymbol{N}_c'\boldsymbol{N}_c'^{\mathrm{t}}\,\mathrm{d}\xi \tag{49}$$

$$\boldsymbol{M}_{dd} = \rho I_p\int_{-1}^{1}\boldsymbol{N}_d\boldsymbol{N}_d^{\mathrm{t}}\,\mathrm{d}\xi \tag{50}$$

Note that the element coordinate system is only a local coordinate system not a moving or rotating coordinate system here. Thus, the element matrices referred to the global coordinate system may be obtained from Eqs. (43)–(50) by using the standard coordinate transformation.

2.8. Equations of motion

The nonlinear equations of motion may be expressed by

$$\boldsymbol{F}^R = \boldsymbol{F}^I + \boldsymbol{F}^D - \boldsymbol{P} = \boldsymbol{0} \tag{51}$$

where $\boldsymbol{F}^R$ is the unbalanced force among the inertia nodal force $\boldsymbol{F}^I$, deformation nodal force $\boldsymbol{F}^D$, and the external nodal force $\boldsymbol{P}$. $\boldsymbol{F}^I$ and $\boldsymbol{F}^D$ are assembled from the element nodal force vectors, which are calculated using Eqs. (18), (35)–(42) first in the current element coordinates and then transformed from element coordinate system to global coordinate system before assemblage using standard procedure.

In this paper, a weighted Euclidean norm of the unbalanced force is employed for the equilibrium iterations, and is given by

$$\frac{\|\boldsymbol{F}^R\|}{\sqrt{N}} \leqslant e_{\mathrm{tol}} \tag{52}$$

where N is number of the equations of the system; e_{tol} is a prescribed value of error tolerance.

3. Numerical procedure

An incremental iterative method based on the Newmark direct integration method [12,27] and the Newton–Raphson method is employed here. The basic steps involved in the numerical solution of Eq. (51) are outlined as follows.

Assume that the dynamic equilibrium configuration at time t_n is known. Let $\dot{\boldsymbol{Q}}_n$ and $\ddot{\boldsymbol{Q}}_n$ denote the nodal velocity and acceleration of the structure at time t_n, respectively. Let $\dot{\boldsymbol{Q}}_{n+1}$ and $\ddot{\boldsymbol{Q}}_{n+1}$ denote the nodal velocity and acceleration at time $t_{n+1} = t_n + \Delta t$, respectively, where Δt is the time step size. $\dot{\boldsymbol{Q}}_{n+1}$ and $\ddot{\boldsymbol{Q}}_{n+1}$ may be obtained by the following incremental-iterative procedure.

Step 1

(a) Choose $\Delta \boldsymbol{Q} = \boldsymbol{0}$ as the initial incremental displacement for the time step at time t_{n+1}.

(b) Calculate the initial nodal velocity and acceleration using the Newmark method for the first iteration:

$$\ddot{\boldsymbol{Q}}^{0}_{n+1} = \frac{-1}{\beta\,\Delta t}\dot{\boldsymbol{Q}}_{n} - \left(\frac{1}{2\beta} - 1\right)\ddot{\boldsymbol{Q}}_{n} \tag{53}$$

$$\dot{\boldsymbol{Q}}^{0}_{n+1} = \dot{\boldsymbol{Q}}_{n} - \Delta t[(1-\gamma)\ddot{\boldsymbol{Q}}_{n} + \gamma\ddot{\boldsymbol{Q}}^{0}_{n+1}] \tag{54}$$

where β and γ are parameters of the Newmark method. In the present study, $\beta = 0.25$ and $\gamma = 0.5$ are employed.

Step 2

(a) Let

$$\ddot{\boldsymbol{Q}}_{n+1} = \ddot{\boldsymbol{Q}}^{0}_{n+1} + \frac{1}{\beta\,\Delta t^{2}}\Delta \boldsymbol{Q}\,, \tag{55}$$

and

$$\dot{\boldsymbol{Q}}_{n+1} = \dot{\boldsymbol{Q}}^{0}_{n+1} + \frac{\gamma}{\beta\,\Delta t}\Delta \boldsymbol{Q} \tag{56}$$

(b) Determine the current element cross section coordinates, element coordinates and element deformation nodal parameters for each element using the $\Delta \boldsymbol{Q}$ and the method described in [15,21].

(c) Extract the global nodal velocity and acceleration vectors corresponding to each element from $\dot{\boldsymbol{Q}}_{n+1}$ and $\ddot{\boldsymbol{Q}}_{n+1}$, and then transform them to the current element coordinates using standard procedure. Then calculate time derivatives of element nodal rotation parameters using Eqs. (15) and (16).

(d) Calculate the element implicit (inertia and deformation) nodal force vectors in the current element coordinates using Eqs. (35)–(42), the element deformation nodal parameters, element nodal velocities and accelerations, and the time derivatives of element nodal rotation parameters just obtained. Then calculate the element explicit nodal force vectors using Eq. (18) and the element implicit nodal force vectors just obtained.

(e) Transform the element explicit nodal force vectors from the current element coordinates to the global coordinates using standard procedure. Then calculate the unbalanced force of the structure (Eq. (51)) from the assemblage of the element explicit nodal force vectors referred to the global coordinates.

(f) Check the convergence criterion given in Eq. (52). If Eq. (52) is satisfied, stop the iteration; otherwise go to next step.

Step 3

(a) Let $\ddot{\boldsymbol{Q}}^{0}_{n+1} = \ddot{\boldsymbol{Q}}_{n+1}$ and $\dot{\boldsymbol{Q}}^{0}_{n+1} = \dot{\boldsymbol{Q}}_{n+1}$.

(b) Calculate the element stiffness and mass matrices in the current element coordinates using Eqs. (43)–(50).

(c) Transform the element stiffness and mass matrices from the current element coordinates to the global coordinates using a standard procedure. Then calculate the structural stiffness matrix and mass matrix $\boldsymbol{K}$ and $\boldsymbol{M}$ from the assemblage of the element stiffness and mass matrices.

(d) Calculate a displacement correction $\Delta \boldsymbol{Q}$ using the Newton–Raphson method:

$$\Delta \boldsymbol{Q} = -\hat{\boldsymbol{K}}^{-1}\boldsymbol{F}^{R} \tag{57}$$

$$\hat{\boldsymbol{K}} = \boldsymbol{K} + \frac{1}{\beta\,\Delta t^{2}}\boldsymbol{M} \tag{58}$$

where $\hat{\boldsymbol{K}}$ is the so-called effective stiffness matrix.

(e) Go back to step 2.

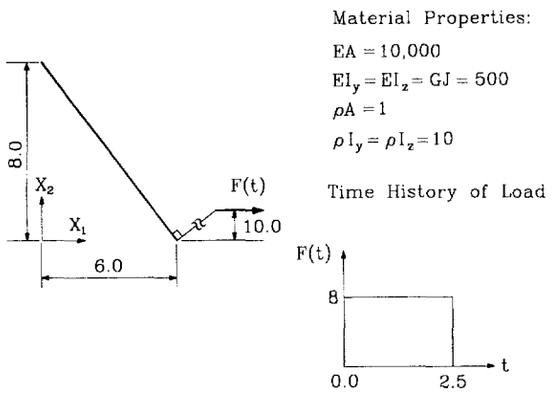

Fig. 3. Flying flexible beam, subjected to conservative force.

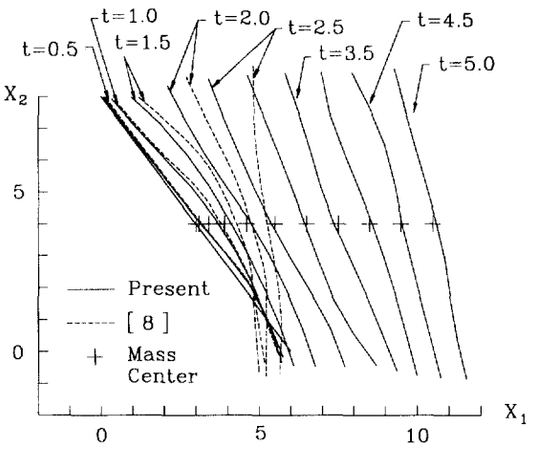

Fig. 4. Sequence of motion of flying flexible beam.

4. Numerical studies

4.1. Flying flexible beam, subjected to conservative force

A flexible beam is initially placed in an inclined position as shown in Fig. 3. A conservative force F is applied at one end of a rigid arm, which is rigidly connected with one end of the flexible beam at another end. The mass of the rigid arm is not considered. The geometry, inertia properties and material properties of the flexible beam and the time history of the conservative force are given in Fig. 3. The beam is analyzed using four and eight elements. The time-step sizes corresponding to four and eight elements are chosen to be 0.1 and 0.01, respectively. The agreement between the results with four elements and those with eight elements are very good. The results, obtained using eight elements, are shown in Fig. 4 together with the solution given in [8], which may be obtained using 10 linear elements. As can be seen, the discrepancy between these two solutions is distinct. The coordinates of the mass center of the flexible beam can be calculated analytically using Newton's second law $\boldsymbol{F} = m\ddot{\boldsymbol{X}}^c$, where $\boldsymbol{F}$ is the external force vector, m is the mass of the flexible beam, and $\boldsymbol{X}^c$ is the position vector of the mass center. The analytical solution of the mass center at different time is also depicted in Fig. 4. The coordinates of the mass center of the flexible beam at different time obtained from the present

Table 1
Coordinates of mass center of flexible beam in Section 4.1

Time	Present (8 ele., $\Delta t = 0.01$)		Present (4 ele., $\Delta t = 0.1$)		Analytical	
	X_1^c	X_2^c	X_1^c	X_2^c	X_1^c	X_2^c
0.0	3.0	4.0	3.0	4.0	3.0	4.0
0.5	3.1001	3.9998	3.0997	4.0004	3.1	4.0
1.0	3.4001	3.9997	3.3988	4.0017	3.4	4.0
1.5	3.9004	3.9996	3.8982	4.0040	3.9	4.0
2.0	4.6008	3.9996	4.6003	4.0046	4.6	4.0
2.5	5.5013	3.9998	5.5089	4.0053	5.5	4.0
3.0	6.5039	4.0002	6.5225	4.0089	6.5	4.0
3.5	7.5061	4.0005	7.5424	4.0140	7.5	4.0
4.0	8.5083	4.0008	8.5623	4.0181	8.5	4.0
4.5	9.5105	4.0007	9.5831	4.0161	9.5	4.0
5.0	10.513	4.0007	10.6049	4.0124	10.5	4.0

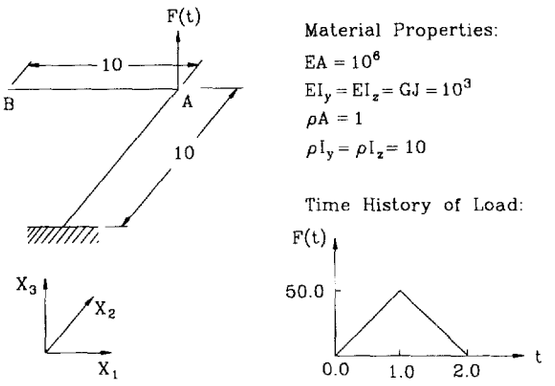

Fig. 5. Right angle cantilever beam.

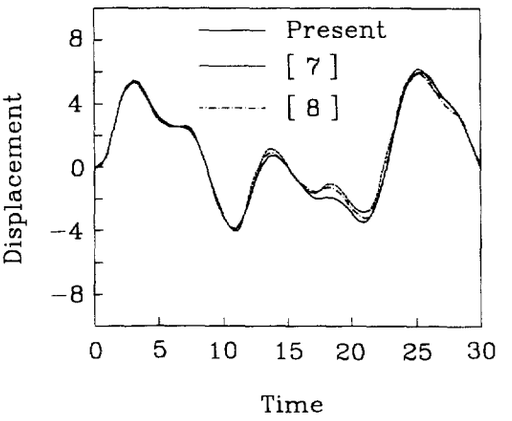

Fig. 6. Time of histories of displacement in the X_1 direction at point A.

numerical results are shown in Table 1 together with the result of analytical solution. It can be seen that the agreement between these two solutions is very good.

4.2. Right angle cantilever beam

The example considered is a right angle cantilever beam subjected to an out-of-plane concentrated load as shown in Fig. 5. The geometry, inertia properties and material properties of the right angle and the load condition are given in Fig. 5. Four elements are used for discretization. A time-step size of $\Delta t = 0.25$ is used. The time histories of out-of-plane displacements of the elbow and the tip are given in Figs. 6 and 7. It is seen that the present results are in excellent agreement with those given in [7] and [8].

4.3. Right angle beam in free flight

This problem has been simulated first by Iura and Atluri [8]. The geometry, inertia properties and material properties of the right angle and the load conditions are given in Fig. 8. The forces F_1 and F_2 are applied at the

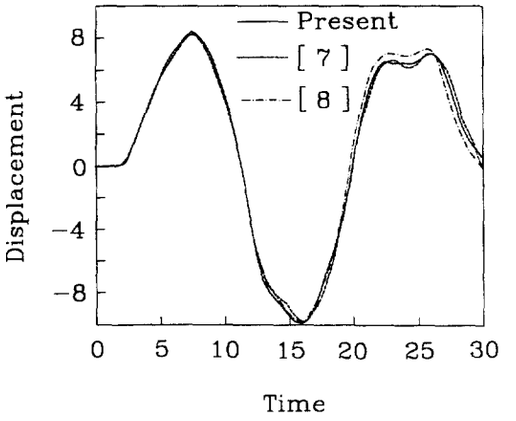

Fig. 7. Time of histories of displacement in the X_3 direction at point B.

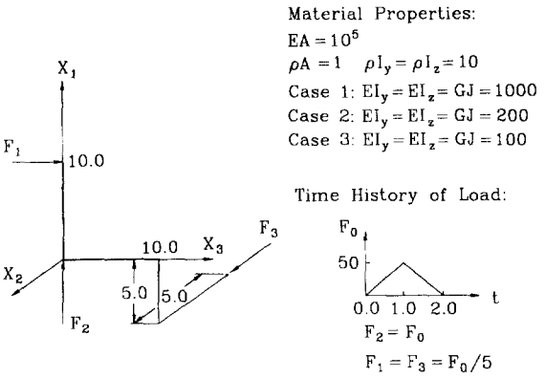

Fig. 8. Right angle beam in free flight.

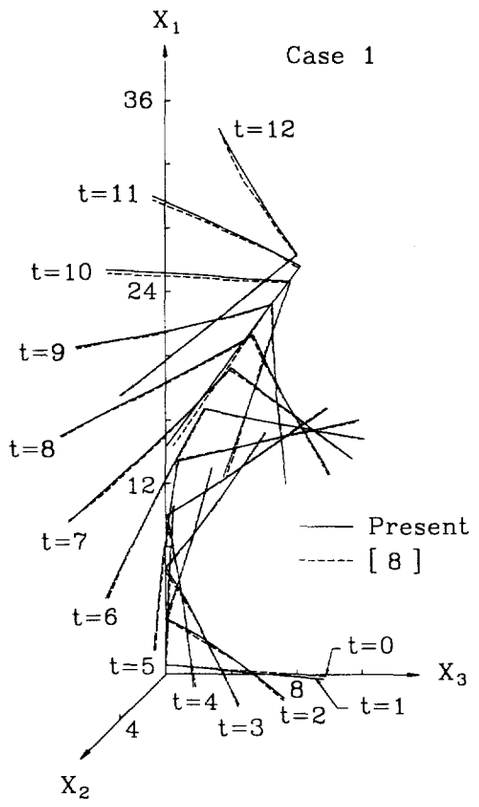

Fig. 9. Sequence of motion for right angle beam in free flight (case 1).

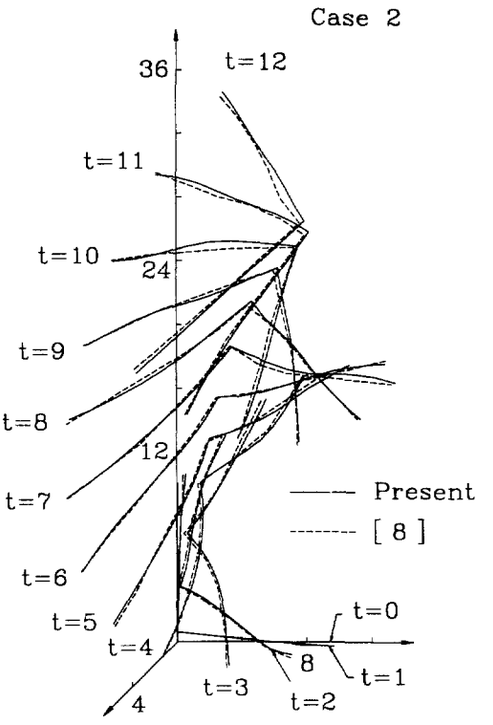

Fig. 10. Sequence of motion for right angle beam in free flight (case 2).

beam axis, while the force F_3 is applied at one end of a rigid arm which is rigidly connected with one end of the flexible right angle at another end.

Three different cases are considered in which the bending and the torsional rigidities are altered. Sixteen elements are used for discretization. A time-step size of $\Delta t = 0.01$ is used. The sequence of motion is depicted in Figs. 9–11. It is seen that the present results are in excellent agreement with those given in [8].

4.4. Flying flexible beam, subjected to triangular pulse force and moments

The flexible beam discussed in Section 4.1 is reconsidered here. This problem was first analyzed in [7]. The beam is initially at an inclined position in the $X_1 - X_2$ plane as shown in Fig. 12. A spatially fixed force along X_1 direction and a spatially fixed moment with X_2 and X_3 components are applied at one end of the beam. The time histories of the magnitude of these applied force and moment are given in Fig. 12. The beam is analyzed using 10 elements. The time step size is chosen to be 0.01. The sequence of motion is depicted in Figs. 13 and 14. In Fig. 13, the trace of both ends of the beam are shown in dot lines. Also shown in Figs. 13 and 14 are the results reported in [7], which are obtained using 10 linear elements and a time step size of $\Delta t = 0.1$. As can be seen, the discrepancy between these two solutions is distinct. The sequence of motion for the mass center of the beam, calculated analytically using Newton's second law at different time, is also shown in Figs. 13 and 14 to verify the accuracy of the present results. The coordinates of the mass center of the flexible beam at different time obtained from the present numerical results are shown in Table 2 together with the result of analytical solution. It can be seen that the agreement between these two solutions is very good.

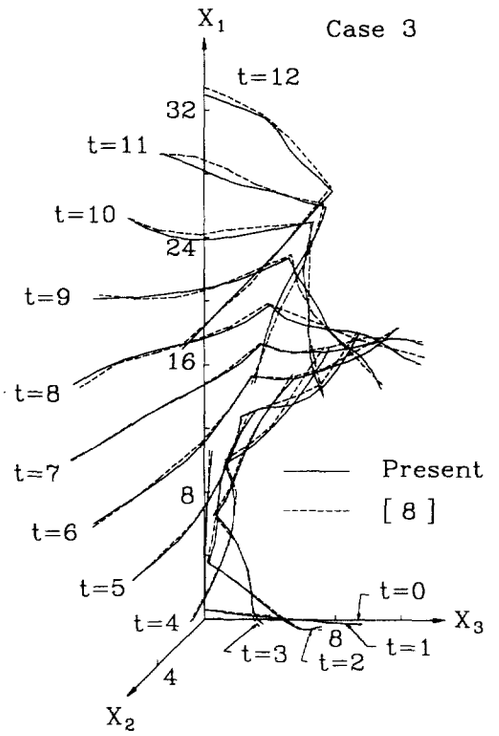

Fig. 11. Sequence of motion for right angle beam in free flight (case 3).

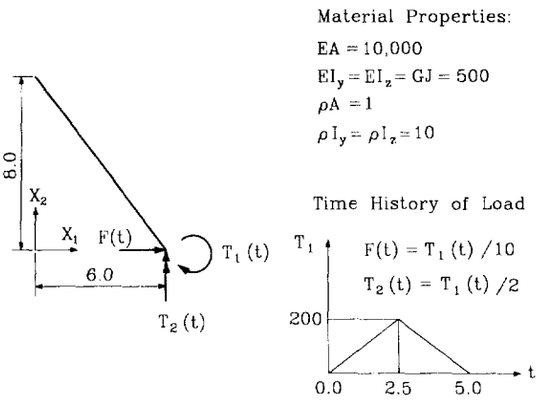

Fig. 12. Flying flexible beam, subjected to triangular pulse force and moments.

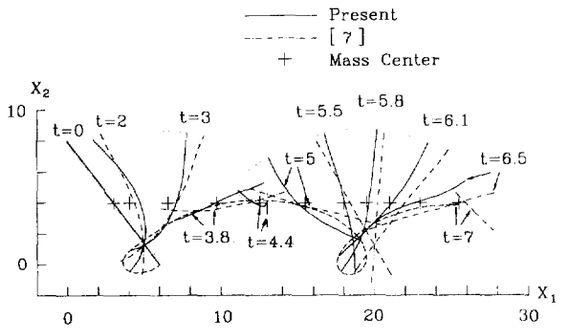

Fig. 13. Sequence of motion of flying flexible beam ($X_1 - X_2$ plane).

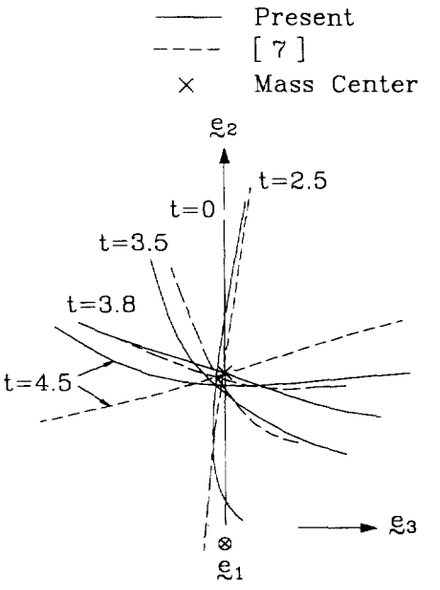

Fig. 14. Sequence of motion of flying flexible beam ($X_2 - X_3$ plane).

Table 2
Coordinates of mass center of flexible beam in Section 4.4

Time	Present			Analytical		
	X_1^c	X_2^c	$X_3^c\,(10^{-3})$	X_1^c	X_2^c	X_3^c
0.0	3.0	4.0	0.0	3.0	4.0	0.0
2.0	4.0659	3.9975	−1.9077	4.0667	4.0	0.0
3.0	6.5548	3.9961	−5.0139	6.5667	4.0	0.0
3.8	9.7007	4.0052	−2.0264	9.7304	4.0	0.0
4.4	12.4845	4.0164	−4.6742	12.5288	4.0	0.0
5.0	15.4386	4.0316	15.9830	15.5000	4.0	0.0
5.5	17.9296	4.0446	25.9090	18.0000	4.0	0.0
5.8	19.4242	4.0503	29.8330	19.5000	4.0	0.0
6.1	20.9173	4.0546	32.4050	21.0000	4.0	0.0
6.5	22.9053	4.0598	35.2470	23.0000	4.0	0.0
7.0	25.3900	4.0667	38.8380	25.5000	4.0	0.0

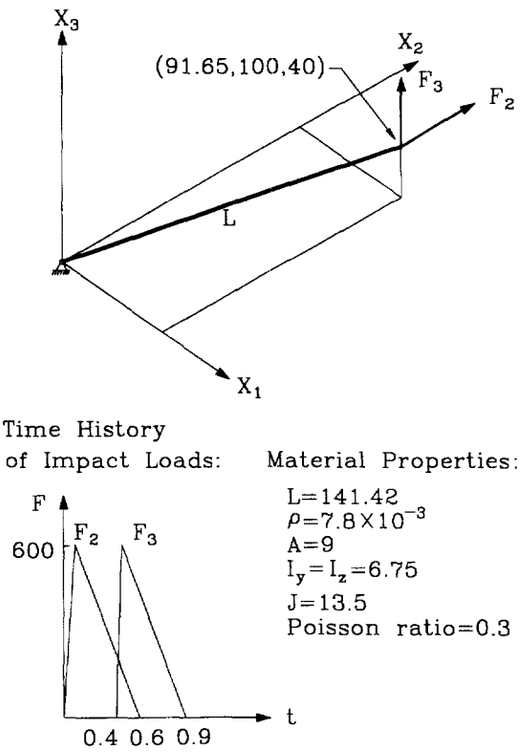

Fig. 15. Articulated-free rod.

4.5. Articulated-free rod

The example considered is an articulated-free rod subjected to two impact loads on its free end as shown in Fig. 15. The rod is articulated to the foundation through a ball joint. Two different Young's modulus of the rod are considered: (a) $E = 2.1 \times 10^9$ and (b) $E = 6.3 \times 10^6$. Five elements are used for discretization. The time step sizes are chosen to be 0.001 and 0.01 for cases (a) and (b), respectively. The time histories of tip coordinates of the rod are given in Figs. 16–19 together with those reported in [10]. Excellent agreement between these two solutions is observed.

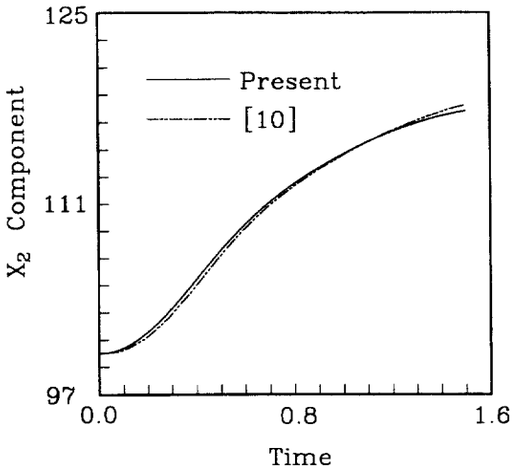

Fig. 16. Y component of the tip coordinates of the rod ($E = 2.1 \times 10^9$).

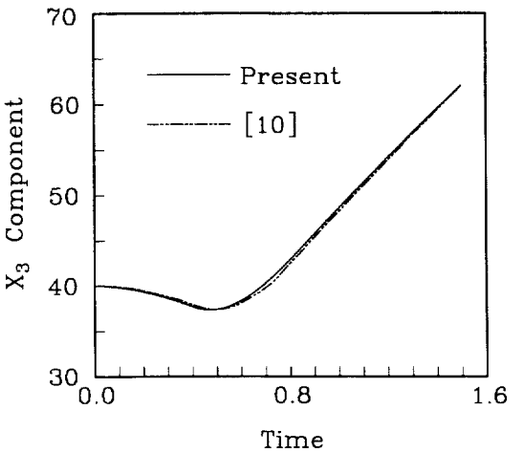

Fig. 17. Z component of the tip coordinates of the rod ($E = 2.1 \times 10^9$).

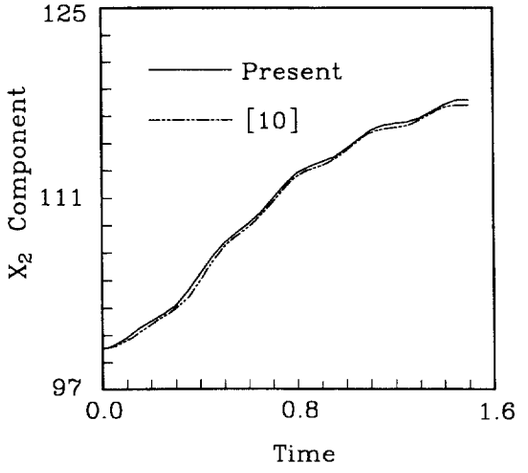

Fig. 18. Y component of the tip coordinates of the rod ($E = 6.3 \times 10^6$).

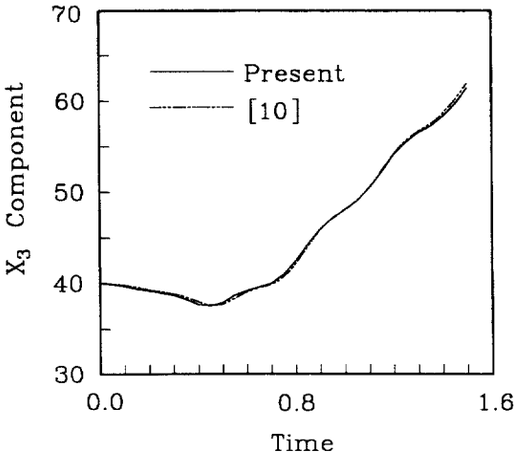

Fig. 19. Z component of the tip coordinates of the rod ($E = 6.3 \times 10^6$).

5. Conclusions

A consistent co-rotational total Lagrangian finite element formulation and numerical procedure for the geometrically nonlinear dynamic analysis of spatial Euler beam with large rotations but small strain is presented.

The nodal coordinates, displacements, rotations, velocities, accelerations and the equations of motion of the structure are defined in a fixed global set of coordinates. The beam element has two nodes with six degrees of freedom per node. The element nodal forces are conventional forces and moments. The kinematics of beam element is defined in terms of element coordinates which are constructed at the current configuration of the beam element. Here, the assumption of Euler beam is properly considered. Both the element inertia and deformation nodal forces are systematically derived by consistent linearization of the fully geometrically nonlinear beam theory by using the d'Alembert principle and the virtual work principle. In conjunction with the co-rotational formulation, the higher order terms of nodal parameters in element nodal forces are consistently neglected. However, in order to include the nonlinear coupling among the bending, twisting and stretching

deformations, the terms up to the second order of nodal parameters are retained in element deformation nodal forces. It should be noted that the element coordinate system is just a local coordinate system, which is updated at each iteration, not a moving coordinate system. Thus, the velocity and acceleration described in the element coordinates are the absolute velocity and acceleration. The element equations are constructed first in the element coordinate system and then transformed to the global coordinate system by using standard procedure.

An incremental-iterative method based on the Newmark direct integration method and the Newton–Raphson method is employed here for the solution of the nonlinear equations of motion. From the numerical examples studied, the accuracy and efficiency of the proposed method is well demonstrated.

It is believed that the consistent co-rotational formulation for beam element and numerical procedure presented here may represent a valuable engineering tool for the dynamic analysis of three-dimensional beam structures.

References

[1] T. Belytschko and B.J. Hsieh, Nonlinear transient finite element analysis with convected coordinates, Int. J. Numer. Methods Engrg. 7 (1973) 255–271.
[2] T. Belytschko and L. Schwer, Large displacement, transient analysis of space frames, Int. J. Numer. Methods Engrg. 11 (1977) 65–84.
[3] K.J. Bathe, E. Ramm and E.L. Wilson, Finite element formulations for large deformation dynamics, Int. J. Numer. Methods Engrg. 9 (1975) 353–386.
[4] A. Rosen, R.G. Loewy and M.B. Mathew, Nonlinear dynamics of slender rods, AIAA J. 25 (1987) 711–619.
[5] J.C. Simo and L. Vu-Quoc, The role of non-linear theories in transient dynamic analysis of flexible structures, J. Sound Vib. 119 (1987) 487–508.
[6] J.C. Simo and L. Vu-Quoc, On the dynamics of flexible beams under large overall motions—The plane case: Part 1 and Part 2, J. Appl. Mech. Engrg. 56 (1986) 217–245.
[7] J.C. Simo and L. Vu-Quoc, On the dynamics in space of rods undergoing large motions—a geometrically exact approach, Comput. Methods Appl. Mech. Engrg. 66 (1988) 125–161.
[8] M. Iura and S.N. Atluri, Dynamic analysis of finitely stretched and rotated three-dimensional space-curved beams, Comput. Struct. 29 (1988) 875–889.
[9] A. Cardona and M. Geradin, A beam finite element non-linear theory with finite rotation, Int. J. Numer. Methods Engrg. 26 (1988) 2403–2438.
[10] A. Cardona and M. Geradin, Modeling of superelements in mechanism analysis, Int. J. Numer. Methods Engrg. 32 (1991) 1565–1593.
[11] K.M. Hsiao and J.Y. Jang, Dynamic analysis of planar flexible mechanisms by co-rotational formulation, Comput. Methods Appl. Mech. Engrg. 87 (1991) 1–14.
[12] K.M. Hsiao, R.T. Yang and A.C. Lee, A consistent finite element formulation for nonlinear dynamic analysis of planar beam, Int. J. Numer. Methods Engrg. 37 (1994) 75–89.
[13] K.M. Hsiao and R.T. Yang, A co-rotational formulation for nonlinear dynamic analysis of curved Euler beam, Comput. Struct. 54 (1995) 1091–1097.
[14] K. Mattiasson and A. Samuelsson, Total and updated Lagrangian forms of the co-rotational finite element formulation in geometrically and materially nonlinear analysis, in: C. Tailor, E. Hinton and D.R.J. Owen, eds., Numerical Methods for Non-linear Problems, Vol. 2 (Pineridge Press, Swansea, UK, 1984) 135–151.
[15] K.M. Hsiao, Corotational total Lagrangian formulation for three-dimensional beam element, AIAA J. 30 (1992) 797–804.
[16] J.H. Argyris, P.C. Dunne and D.W. Scharpf, On large displacement–small strain analysis of structures with rotation degree of freedom, Comput. Methods Appl. Mech. Engrg. 14 (1978) 401–451; 15 (1978) 99–135.
[17] J.H. Argyris, O. Hilpert, G.A. Malejannakis and D.W. Scharpf, On the geometrical stiffness of a beam in space—A consistent v.w. approach, Comput. Methods Appl. Mech. Engrg. 20 (1979) 105–131.
[18] J.H. Argyris, H. Balmer, J.St. Doltsinis, P.C. Dunne, M. Haase, M. Kleiber, G.A. Malejannakis, H.P. Mlejenek, M. Muller and D.W. Scharpf, Finite element method—the natural approach, Comput. Methods Appl. Mech. Engrg. 17/18 (1979) 1–106.
[19] J.H. Argyris, B. Boni, U. Hindenlang and M. Kleiber, Finite element analysis of two- and three-dimensional elasto-plastic frames—The natural approach, Comput. Methods Appl. Mech. Engrg. 35 (1982) 221–248.
[20] J.H. Argyris, An excursion into large rotation, Comput. Methods Appl. Mech. Engrg. 32 (1982) 85–155.
[21] K.M. Hsiao and C.M. Tsay, A motion process for large displacement analysis of spatial frames, Int. J. Space Struct. 6 (1991) 133–139.
[22] H. Goldstein, Classical Mechanics (Addison-Wesley, Reading, MA, 1980).
[23] M. Borri, F. Mello and S.N. Atluri, Variational approaches for dynamics and time-finite-elements: numerical studies, Comput. Mech. 7 (1990) 49–76.
[24] D.J. Dawe, Matrix and Finite Element Displacement Analysis of Structures (Oxford University, NY, 1984).
[25] T.J. Chung, Continuum Mechanics (Prentice-Hall, Englewood Cliffs, NJ, 1988).
[26] K.M. Hsiao, H.J. Horng and Y.R. Chen, A corotational procedure that handles large rotations of spatial beam structures, Comput. Struct. 27 (1987) 769–781.
[27] K.J. Bathe, Finite Element Procedure in Engineering Analysis (Prentice-Hall, Englewood Cliffs, NJ, 1982).